Frontiers of Physics
https://doi.org/10.1007/s11467-018-0860-5
Front. Phys.
14(1), 13604 (2019)

RESEARCH ARTICLE

Hydrothermal synthesis, structure and magnetic properties of Ru doped $La_{0.5}Sr_{0.5}MnO_3$

Ling-Ling Wang[1], Jia-Nan Chu[1,2,3], Xuan Zhang[1,4], Yong-Hui Ma[1,2,3], Qiu-Cheng Ji[1,2], Wei Li[5], Hui Zhang[1,2], Gang Mu[1,2,†], Xiao-Ming Xie[1,2,3]

[1] *State Key Laboratory of Functional Materials for Informatics, Shanghai Institute of Microsystem and Information Technology, Chinese Academy of Sciences, Shanghai 200050, China*
[2] *CAS Center for Excellence in Superconducting Electronics (CENSE), Shanghai 200050, China*
[3] *University of Chinese Academy of Sciences, Beijing 100049, China*
[4] *Shanghai Key Laboratory of High Temperature Superconductors, Shanghai University, Shanghai 200444, China*
[5] *State Key Laboratory of Surface Physics and Department of Physics, Fudan University, Shanghai 200433, China*
Corresponding author. Email: †mugang@mail.sim.ac.cn
Received June 1, 2018; accepted August 14, 2018

Synthesis, structure and magnetic properties of Ru doped perovskite structured manganite $La_{0.5}Sr_{0.5}MnO_3$ were investigated experimentally. A hydrothermal method was used for the preparation of the samples. A high-temperature annealing process was also employed to make a comparison. A slightly enhancement of the unit cell volume was observed with the increase of Ru concentration. Scanning electron microscopy shows that the materials are made up of cube-shaped particles with dimension of several micrometers. Importantly, it is found that both the Curie temperature T_C and saturation moment can be reduced by Ru doping. The value of coercive field is not affected by the introduction of Ru.

Keywords $La_{0.5}Sr_{0.5}MnO_3$, hydrothermal synthesis, Ru doping, Curie temperature

1 Introduction

Transition metal compounds with the perovskite structure were investigated extensively for several decades, since the discovery of high-temperature superconductivity in cuprates [1]. The manganite (La,Sr)MnO_3 and other analogues, also with the perovskite structure, were studied for many years due to the colossal magnetoresistance (CMR) which has potential applications in magnetic devices [2–7]. Besides the CMR feature, this system also shows a rather complicated magnetic behavior and crystal structure with the variation of the chemical compositions [8–10]. The physical properties can also be tuned by chemical doping on the site of Mn [11–21]. However, the influence of the dopants on the physical properties is rather controversial. For example, the Curie temperature T_C was found to decrease with Ru doping by some researchers [15–17], while an enhancement of T_C was also reported by other groups [18, 19]. So these issues need to be clarified by more reliable experiments.

The solid-state reaction method at the temperature above 1200°C was used widely to synthesize the polycrystalline samples of (La,Sr)MnO_3 [17–19]. Later on, a mild hydrothermal method under low temperature was also developed [22–24]. Besides the simplicity of the synthesis procedures and the low energy consumption, hydrothermal method also shows advantages in improving the homogeneity of the samples, especially controlling the oxygen content [23]. It was found that the chemical composition of the hydrothermal samples is close to the ideal value and the deviation of oxygen is only about 1% for $La_{0.5}Sr_{0.5}MnO_3$ [23]. This is important for the fundamental research and may facilitate the obtaining of intrinsic properties. To our knowledge, there is no reports on the Ru doped $La_{0.5}Sr_{0.5}MnO_3$ by the hydrothermal method.

In this paper, we report the hydrothermal synthesis, structure characterization, and physical investigations of Ru doped $La_{0.5}Sr_{0.5}MnO_3$. With the increase of Ru doping, the *c*-axis lattice constant increases slightly while the *a*-axis lattice remains unchanged. Both the Curie temperature T_C and saturation moment are suppressed by Ru doping. A comparative experiment was also conducted by annealing one hydrothermal sample at high temperature.

2 Experiments

$La_{0.5}Sr_{0.5}Mn_{1-x}Ru_xO_3$ ($x = 0$, 0.1, 0.2, 0.3) samples was synthesized by hydrothermal method. In a typical synthesis, 1.75 mmol $MnCl_2{\cdot}4H_2O$, 1.25 mmol $SrCl_2{\cdot}6H_2O$, 1.25 mmol $La(NO_3)_3{\cdot}6H_2O$, 0.75 mmol $KMnO_4$ were suc-

cessively added into the 15 mL deionized water by stirring for 30 minutes and then KOH as a mineralizer was slowly added with continued stirring for 60 minutes. Finally, the solution was poured into 25 mL Teflon-lined autoclave and heated to 240°C for 40 hours. The reacted precipitate was cleaned with deionized water and ethanol several times and then dried at 80°C for 24 h. The dried black powder is polycrystalline $La_{0.5}Sr_{0.5}MnO_3$, along with a small amount of $La(OH)_3$. The Ru doped $La_{0.5}Sr_{0.5}Mn_{1-x}Ru_xO_3$ ($x = 0.1$, 0.2, 0.3) were obtained by partially replacing the reagent $KMnO_4$ with $KRuO_4$ appropriately. In order to have a comparison, the hydrothermally synthesized samples were annealed at high temperature: $La_{0.5}Sr_{0.5}Mn_{1-x}Ru_xO_3$ powders with small amounts of $La(OH)_3$ were cold pressed into pellets and thermally treated at 1000°C for 24 hours in air.

The actual Ru concentrations were checked and determined by the energy dispersive X-ray spectroscopy (EDS) measurements on an Oxford Instruments device. The crystal structure was checked by powder X-ray diffraction (PXRD) measurements at room temperature using a DX-2700 diffractometer with Cu K_α radiation. The morphology of the samples was characterized by JSM-6510 scanning electron microscope (SEM). The magnetic properties were measured on a Quantum Design magnetic property measurement system (MPMS).

3 Results and discussion

3.1 Composition, morphology and structure

The actual doping levels of the samples were analyzed and determined by the energy dispersive X-ray spectroscopy (EDS) measurements. The results can be seen in Table 1. The Ru concentration determined from EDS measurements, x_{EDS}, will be used in the following discussions of the present paper.The morphology of the hydrothermal samples with $x_{EDS} = 0$ and 0.066 were evaluated by SEM. As shown in Fig. 1, the material is made up of cube shaped particles with typical dimension 5–10 μm, which is quite similar with that previous reported by Spooren *et al.* [23].

As shown in Fig. 2(a), both the X-ray and neutron diffraction experiments have revealed a distorted perovskite structure in $La_{0.5}Sr_{0.5}MnO_3$ [8, 23]. Here we examined the crystal structure of our samples by the PXRD measurements. The PXRD patterns of hydrothermal $La_{0.5}Sr_{0.5}Mn_{1-x}Ru_xO_3$ ($x_{EDS} = 0$, 0.066, 0.082, 0.136), along with the annealed sample with $x_{EDS} = 0$, were showed in Fig. 2(b). Obviously all the hydrothermal samples are accompanied by a small amount of $La(OH)_3$ as indexed by the asterisks, which rises gradually with the increase of Ru concentration. In the annealed sample, $La(OH)_3$ is absent and small amounts of La_2O_3 can be observed.

Table 1 Actual Ru concentrations and lattice constants for three hydrothermal (abbreviate as Hy-) $La_{0.5}Sr_{0.5}Mn_{1-x}Ru_xO_3$ ($x = 0$, 0.1, 0.2, 0.3) materials and one annealed (abbreviate as An-) sample ($x = 0$).

Materials	x_{EDS}	a (Å)	c (Å)	V (Å^3)
An- $x = 0$	0	5.43918	7.73798	228.926
Hy- $x = 0$	0	5.43579	7.73213	228.468
Hy- $x = 0.1$	0.066	5.43624	7.76826	229.573
Hy- $x = 0.2$	0.082	5.43535	7.77670	229.747
Hy- $x = 0.3$	0.136	–	–	–

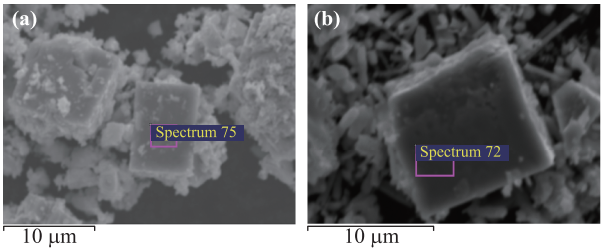

Fig. 1 Scanning electron micrographs of hydrothermal $La_{0.5}Sr_{0.5}Mn_{1-x}Ru_xO_3$ with $x_{EDS} = 0$ **(a)** and 0.066 **(b)**.

$La(OH)_3$ is the major impurity in the process of hydrothermal synthesis. It has been reported that the hydrothermal temperature and reaction time have significant influences on the products [24]. During the process of heating, the $La(OH)_3$ nucleus begin to appear and form nanocrystals around 180°C [25]. With the prolongation of reaction time and the increasing of temperature, the $La(OH)_3$ nanorods release La^{3+} ions, which provide enough elements for the formation of $La_{0.5}Sr_{0.5}MnO_3$ crystals [24]. In this meaning, higher temperature or longer reaction time is beneficial to decrease the number of $La(OH)_3$ nanorods. We have tried longer reaction time (40 and 60 hours) and no differences can be found compared with 24 h. As for the reaction temperature,

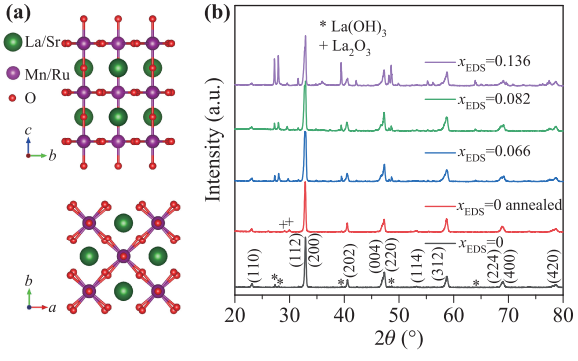

Fig. 2 **(a)** A sketch map of the crystal structure of $La_{0.5}Sr_{0.5}Mn_{1-x}Ru_xO_3$. It is a distorted perovskite structure. **(b)** X-ray diffraction patterns for $La_{0.5}Sr_{0.5}Mn_{1-x}Ru_xO_3$ samples with different doping levels. One can see that all the main peaks can be indexed to the tetragonal structure with the space group I4/mcm. The impurity phases were identified to be $La(OH)_3$ and La_2O_3.

Spooren *et al.* [23] showed that 240°C is enough to prepare $La_{0.5}Sr_{0.5}MnO_3$. Thus, the reaction condition was fixed to 240°C and 24 h in our experiment. In addition, we found the formation of $La_{0.5}Sr_{0.5}MnO_3$ crystals can be affected by the amount of KOH. The samples were not produced when the concentration of KOH was lower than 6 mol/L.

The (004) and (220) peaks overlap in the samples with $x_{EDS} = 0$ and separate gradually when the Ru doping content is increased stage by stage. Similar behaviors can been observed for the (224) and (400) peaks. These features can be understood in terms of the different evolution tendencies of *a*- and *c*-axis lattice constants with Ru doping. It is also found that the (114) peak is weakened and disappear finally with increasing Ru content. This change has been reported by other group and ascribed to influence of Ru ionic substitution [18]. In addition, the raw data of PXRD was analyzed by PowderX software [26]. It indicates that all the polycrystalline samples have a tetragonal structure with I4/mcm space group. The obtained lattice constants are showed in Table 1. For the hydrothermal sample without Ru doping, the lattice constants are consistent with other reports on hydrothermal $La_{0.5}Sr_{0.5}MnO_3$ [23], which indicates that the actual Sr content of our samples is also around 0.5. With increasing Ru contents, the *c*-axis lattice constants increase, while the *a*-axis lattice remains almost unchanged. The unit cell volume becomes larger for the Ru doped samples. The content of impurity for the sample with $x_{EDS} = 0.136$ is rather high, which prevents obtaining the accurate lattice constants for this sample.

3.2 Magnetic properties

Figure 3 shows the temperature dependence of magnetization (M–T) for the hydrothermal $La_{0.5}Sr_{0.5}Mn_{1-x}Ru_xO_3$ ($x_{EDS} = 0$, 0.066, 0.082, 0.136) and the annealed sample with $x_{EDS} = 0$. Both the zero-field-cooled (ZFC) and field-cooling (FC) magnetization with applied field 100 Oe were measured from 2 K up to 400 K. With the temperature decreasing, all the M–T curves undergo a transition from paramagnetic(PM) to ferromagnetic(FM) states. Note that the presence of impurity should have influences on the magnitude of the magnetization data per unit mass, nevertheless the FM transition is not affected because $La(OH)_3$ does not show any magnetic transition in the temperature range we measured. The Curie temperature T_C was defined as the intersection point of two trendlines below and above the transition in M–T curve, as shown by the blue arrow in Fig. 3. The obtained values of T_C as a function of Ru concentration were shown in Fig. 5. We will discuss the detailed behaviors later.

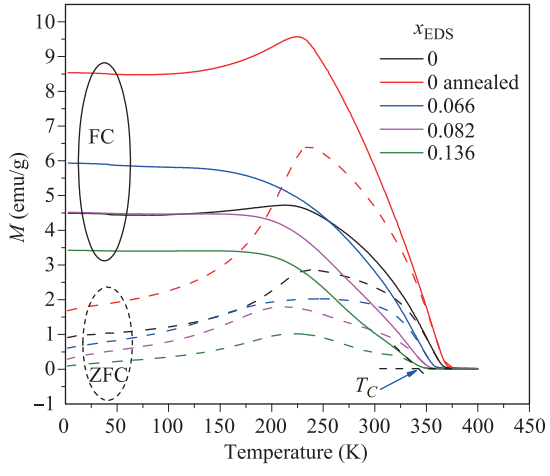

Fig. 3 Temperature dependent magnetic moment (M–T) data of the hydrothermal samples with $x_{EDS} = 0$, 0.066, 0.082, 0.136 and the annealed sample with $x_{EDS} = 0$. The applied field is 100 Oe. Both the zero-field-cooling (ZFC) and field-cooling (FC) data are shown.

The field dependence of magnetization (M–H) measurements were performed for all the four samples at 5 K with the external field from 0 to 6 T and the results were plotted in Fig. 4. The value of magnetization (M) increases rapidly under low field and then inclines to saturation with the increase of field, exhibiting a spontaneous magnetizing process. This is consistent with the results of M–T measurements and indicates a ferromagnetic ground state in low temperature. From the hysteresis loop, the saturation moments can be calculated. We find that for the hydrothermal samples, the magnetic moments were reduced from 1.15 μ_B for the undoped compound to 0.56 μ_B for the compound with $x = 0.082$. The annealed sample has a larger moment of 1.44 μ_B. We note that the accuracy of the estimated magnetic moments was weakened by the presence of $La(OH)_3$ impurities. As can be seen in an enlarged view of the data in the inset of Fig. 4, the coercive field is about 400 Oe and remains almost unchanged with Ru doping for the hydrothermal samples. The annealed sample shows a smaller coercive field of about 300 Oe.

As shown in Fig. 5, with the increase of Ru concentration, the Curie temperature T_C is suppressed, indicating

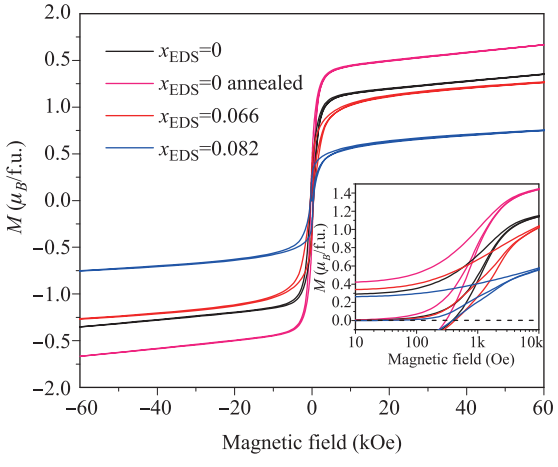

Fig. 4 The magnetization as a function of the applied magnetic field for four samples. The inset shows an enlarged view in the low-field range.

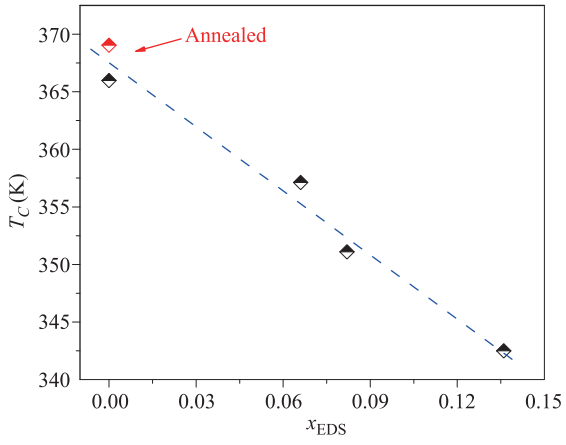

Fig. 5 Variation of Curie temperature T_C as a function of Ru concentration x_{EDS}. The dashed line is a guide for eyes.

the destructive effect on the FM order induced by Ru doping. Such a tendency is consistent with the substitution of most other elements for Mn ions [11–14]. For the Ru substitution, just as we have mentioned in the introduction, the existing experimental results are still rather controversial. The results of Sahu *et al.* [15], Wang *et al.* [16], and Zaidi *et al.* [17] revealed the same tendency as our observations. Meanwhile, Ying *et al.* [18] and Saber *et al.* [19] reported the opposite behaviors upon Ru doping. Moreover, no significant change in T_C as a function of Ru doping was found in the experiments of Dhiman *et al.* [20]. These reports along with our result are summarized in Table 2 for clarity. One possible reason for such scattering experimental results is the complex magnetic phase diagram of this system. The type and strength of the magnetic interactions may be different with the variation of rare-earth elements (La, Sm, ...), alkaline-earth elements (Ba, Sr, Ca, ...), and even the alkaline-earth element concentration. Another noteworthy factor is the difficulty in the precise controlling of the Sr concentration and oxygen content in preparing the samples under the condition of high temperature. The low-temperature hydrothermal synthesis supplied a scheme to achieve a more reliable result of this issue. It was found that the compound with La:Sr = 1:1 is rather stable and $La_{0.5}Sr_{0.5}MnO_3$ was always produced even the amount of the reagent was modified [23]. In addition, the Curie temperature does not change among samples with different amount of impurity $La(OH)_3$ prepared in different hydrothermal conditions [24]. So the effect of Ru doping in our present work was achieved on a more solid foundation. As can be seen from our comparative experiment, the behavior of the annealed sample deviated from that of the hydrothermal samples in terms of lattice constants, Curie temperature, saturation moment, and coercive field, possibly originating from the variation of Sr and oxygen contents during the high-temperature annealing process. The annealed samples with Ru doping showed some indications of phase separation and the data were not shown in this paper.

Table 2 Summary of reported results for the Ru-doping effects on T_C in (La, Sr) MnO_3 and related compounds.

Materials	Ru-doping effect on T_C*	Ref.
$La_{0.6}Pb_{0.4}MnO_3$	↘	[15]
$La_{0.7}Sr_{0.3}MnO_3$	↘	[16]
$La_{0.6}Pr_{0.1}Sr_{0.3}MnO_3$	↘	[17]
$La_{0.5}Sr_{0.5}MnO_3$	↗	[18]
$Sm_{0.55}Sr_{0.45}MnO_3$	↗	[19]
$La_{0.5}Ca_{0.5}MnO_3$	⟶	[20]
$La_{0.5}Sr_{0.5}MnO_3$	↘	This work

*↘: Suppresses T_C. ↗: Enhances T_C. ⟶: No changes.

4 Conclusion

In conclusion, we have reported the experimental investigations on the hydrothermal synthesis, structural, and magnetic properties of the Ru doped manganite $La_{0.5}Sr_{0.5}MnO_3$ with a distorted perovskite structure. The crystal lattice expanded slightly with the increase of Ru doping. The destructive effect on the FM order by Ru doping was observed: both the Curie temperature T_C and saturation moment are suppressed with the introduction of Ru elements on the site of Mn. The coercive field remains almost unchanged by Ru doping. The behavior of the annealed sample deviated from that of the hydrothermal samples, indicating the subtle different in the detailed compositions due to the high-temperature treatment.

Acknowledgements This work was supported by the Youth Innovation Promotion Association of the Chinese Academy of Sciences (Grant No. 2015187) and the National Natural Science Foundation of China (Grant No. 11204338).

References

1. J. G. Bednorz and K. A. Mäuller, Possible high T_C superconductivity in the Ba-La-Cu-O system, *Z. Phys. B* 64, 189 (1986)
2. R. von Helmolt, J. Wecker, B. Holzapfel, L. Schultz, and K. Samwer, Giant negative magnetoresistance in perovskitelike $La_{2/3}Ba_{1/3}MnO_x$ ferromagnetic films, *Phys. Rev. Lett.* 71(14), 2331 (1993)
3. K. Chahara, T. Ohno, M. Kasai, and Y. Kozono, Magnetoresistance in magnetic manganese oxide with intrinsic antiferromagnetic spin structure, *Appl. Phys. Lett.* 63(14), 1990 (1993)
4. S. Jin, T. H. Tiefel, M. McCormack, R. A. Fastnacht, R. Ramesh, and L. H. Chen, Thousandfold change in re-

sistivity in magnetoresistive La-Ca-Mn-O Films, *Science* 264(5157), 413 (1994)

5. M. McCormack, S. Jin, T. H. Tiefel, R. M. Fleming, J. M. Phillips, and R. Ramesh, Very large magnetoresistance in perovskite-like La-Ca-Mn-O thin films, *Appl. Phys. Lett.* 64(22), 3045 (1994)
6. P. Schiffer, A. P. Ramirez, W. Bao, and S. W. Cheong, Low temperature magnetoresistance and the magnetic phase diagram of $La_{1-x}Ca_xMnO_3$, *Phys. Rev. Lett.* 75(18), 3336 (1995)
7. A. Urushibara, Y. Moritomo, T. Arima, A. Asamitsu, G. Kido, and Y. Tokura, Insulator-metal transition and giant magnetoresistance in $La_{1-x}Sr_xMnO_3$, *Phys. Rev. B* 51(20), 14103 (1995)
8. A. Sundaresan, P. L. Paulose, R. Mallik, and E. V. Sampathkumaran, Bandwidth-controlled magnetic and electronic transitions in $La_{0.5}Ca_{0.5-x}Sr_xMnO_3$ ($0 <\sim x <\sim 0.5$) distorted perovskite, *Phys. Rev. B* 57(5), 2690 (1998)
9. O. Chmaissem, B. Dabrowski, S. Kolesnik, J. Mais, J. D. Jorgensen, and S. Short, Structural and magnetic phase diagrams of $La_{1-x}Sr_xMnO_3$ and $Pr_{1-y}Sr_yMnO_3$, *Phys. Rev. B* 67(9), 094431 (2003)
10. C. Autret-Lambert, M. Gervais, S. Roger, F. Gervais, M. Lethiecq, N. Raimboux, and P. Simon, Inhomogeneous magnetism studied by ESR in $La_{1-x}Sr_xMnO_3$ ($0.45 \leq x \leq 0.62$), *Solid State Sci.* 71, 139 (2017)
11. A. Maignan, C. Martin, and B. Raveau, Substitution of manganese by trivalent and tetravalent elements in the CMR perovskites $Pr_{1-x}(Ca, Sr)_xMnO_3$, *Z. Phys. B* 102, 19 (1996)
12. K. Ghosh, S. B. Ogale, R. Ramesh, R. L. Greene, T. Venkatesan, K. M. Gapchup, R. Bathe, and S. I. Patil, Transition-element doping effects in $La_{0.7}Ca_{0.3}MnO_3$, *Phys. Rev. B* 59(1), 533 (1999)
13. M. Rubinstein, D. J. Gillespie, J. E. Snyder, and T. M. Tritt, Effects of Gd, Co, and Ni doping in $La_{2/3}Ca_{1/3}MnO_3$: Resistivity, thermopower, and paramagnetic resonance, *Phys. Rev. B* 56(9), 5412 (1997)
14. Y. Sun, X. Xu, L. Zheng, and Y. Zhang, Effects of Ga doping in the colossal magnetoresistance material $La_{0.67}Ca_{0.33}MnO_3$, *Phys. Rev. B* 60(17), 12317 (1999)
15. R. K. Sahu and S. S. Manoharan, A Zener pair effect in lanthanum rutheno manganite, *J. Appl. Phys.* 91(10), 7517 (2002)
16. L. M. Wang, J. H. Lai, J. I. Wu, Y. K. Kuo, and C. L. Chang, Effects of Ru substitution for Mn on $La_{0.7}Sr_{0.3}MnO_3$ perovskites, *J. Appl. Phys.* 102(2), 023915 (2007)
17. N. Zaidi, S. Mnefgui, J. Dhahri, and E. K. Hlil, Effect of Ru substitution on the physical properties of $La_{0.6}Pr_{0.1}Sr_{0.3}Mn_{1-x}Ru_xO_3$ ($x = 0.00$, 0.05 and 0.15) perovskites, *RSC Adv.* 5, 31901 (2015)
18. Y. Ying, J. Fan, L. Pi, Z. Qu, W. Wang, B. Hong, S. Tan, and Y. Zhang, Effect of Ru doping in $La_{0.5}Sr_{0.5}MnO_3$ and $La_{0.45}Sr_{0.55}MnO_3$, *Phys. Rev. B* 74(14), 144433 (2006)
19. M. M. Saber, M. Egilmez, A. I. Mansour, I. Fan, K. H. Chow, and J. Jung, Evolution of Curie-Weiss behavior and cluster formation temperatures in Ru-doped $Sm_{0.55}Sr_{0.45}MnO_3$ manganites, *Phys. Rev. B* 82(17), 172401 (2010)
20. I. Dhiman, A. Das, A. K. Nigam, and U. Gasser, Influence of B-site disorder in $La_{0.5}Ca_{0.5}Mn_{1-x}B_xO_3$ (B = Fe, Ru, Al and Ga) manganites, *J. Phys.: Condens. Matter* 23(24), 246006 (2011)
21. Y. Ying, J. Zheng, L. Qiao, W. Li, W. Cai, S. Che, L. Jiang, J. Fan, and M. Lin, Double exchange interaction between Mn^{3+} and Ru^{4+} ions in $La_{1-x}Sr_xMn_{1-x}Ru_xO_3$, *J. Superconduct. Novel Magnet.* 28(10), 3117 (2015)
22. D. Zhu, H. Zhu, and Y. Zhang, Microstructure and magnetization of single-crystal perovskite manganites nanowires prepared by hydrothermal method, *J. Cryst. Growth* 249(1–2), 172 (2003)
23. J. Spooren, R. I. Walton, and F. Millange, A study of the manganites $La_{0.5}M_{0.5}MnO_3$ (M = Ca, Sr, Ba) prepared by hydrothermal synthesis, *J. Mater. Chem.* 15(15), 1542 (2005)
24. Y. Cheng, J. Dai, X. Zhu, D. Wu, and Y. Sun, Preparation, magnetic and microwave absorption properties of $La_{0.5}Sr_{0.5}MnO_3/La(OH)_3$ composites, *Mater. Res. Bull.* 45(6), 663 (2010)
25. B. Tang, J. Ge, and L. Zhuo, The fabrication of $La(OH)_3$ nanospheres by a controllable-hydrothermal method with citric acid as a protective agent, *Nanotechnology* 15(12), 1749 (2004)
26. C. Dong, *PowderX*: Windows-95-based program for powder X-ray diffraction data processing, *J. Appl. Cryst.* 32(4), 838 (1999)